Bifurcation phenomena and dynamo effect in electrically conducting fluids

F. Feudel, S. Rüdiger, N. Seehafer

Institut für Physik, Universität Potsdam,
PF 601553, D-14415 Potsdam, Germany

Abstract. Electrically conducting fluids in motion can act as self-excited dynamos. The magnetic fields of celestial bodies like the Earth and the Sun are generated by such dynamos. Their theory aims at modeling and understanding both the kinematic and dynamic aspects of the underlying processes. Kinematic dynamo models, in which for a prescribed flow the linear induction equation is solved and growth rates of the magnetic field are calculated, have been studied for many decades. But in order to get consistent models and to take into account the back-reaction of the magnetic field on the fluid motion, the full nonlinear system of the magnetohydrodynamic (MHD) equations has to be studied. It is generally accepted that these equations, i.e. the Navier-Stokes equation (NSE) and the induction equation, provide a theoretical basis for the explanation of the dynamo effect. The general idea is that mechanical energy pumped into the fluid by heating or other mechanisms is transferred to the magnetic field by nonlinear interactions. For two special helical flows which are known to be effective kinematic dynamos and which can be produced by appropriate external mechanical forcing, we review the nonlinear dynamo properties found in the framework of the full MHD equations. Specifically, we deal with the ABC flow (named after Arnold, Beltrami and Childress) and the Roberts flow (after G. O. Roberts). The appearance of generic dynamo effects is demonstrated. Applying special numerical bifurcation-analysis techniques to high-dimensional approximations in Fourier space and varying the Reynolds number (or the strength of the forcing) as the relevant control parameter, qualitative changes in the dynamics are investigated. We follow the bifurcation sequences until chaotic states are reached. The transitions from the primary flows with vanishing magnetic field to dynamo-active states are described in particular detail. In these processes the stagnation points of the flows and their heteroclinic connections play a promoting role for the magnetic field generation. By the example of the Roberts flow we demonstrate how the break up of the heteroclinic lines after the primary bifurcation leads to a complicated intersection of stable and unstable manifolds forming a chaotic web which is in turn correlated with the spatial appearance of the dynamo.

1 Introduction to the dynamo problem

The generation and maintenance of magnetic fields by the motion of electrically conducting fluids is the subject of dynamo theory. One of its main objectives is to explain the existence of long lasting cosmical magnetic fields, as for instance, those of the Earth and the Sun. Realistic models, describing the dynamo processes, are given in the form of a complex system of nonlinear partial differential equations including the Navier-Stokes equations (NSE), the induction equation, the heat equation, and the thermodynamic equation of state. Heating causes fluid motions which in turn, notably in the presence of rotation, induce magnetic fields. For a comprehensive account of dynamo theory we refer to Refs. [1–3].

Because of the complexity of realistic models and due to restricted computer capacities, which allow only short time simulations, the dynamo processes are not completely understood yet. In order to get a tractable model, it is generally accepted that the nonlinear system of the incompressible magnetohydrodynamic (MHD) equations contains the basic elements of a dynamo [1]. It consists of the coupled system NSE for the flow and induction equation for the magnetic field in the form

$$\frac{\partial \mathbf{v}}{\partial t} + (\mathbf{v} \cdot \nabla)\mathbf{v} = R^{-1}\nabla^2\mathbf{v} - \nabla p - \frac{1}{2}\nabla\mathbf{B^2} + (\mathbf{B} \cdot \nabla)\mathbf{B} + \mathbf{f}, \tag{1}$$

$$\frac{\partial \mathbf{B}}{\partial t} + (\mathbf{v} \cdot \nabla)\mathbf{B} = Rm^{-1}\nabla^2\mathbf{B} + (\mathbf{B} \cdot \nabla)\mathbf{v}, \tag{2}$$

$$\nabla \cdot \mathbf{v} = \mathbf{0}, \quad \nabla \cdot \mathbf{B} = \mathbf{0}, \tag{3}$$

where $\mathbf{v}$, p, and $\mathbf{B}$ denote fluid velocity, thermal pressure, and magnetic field, R and Rm the kinetic and magnetic Reynolds number, respectively, and $\mathbf{f}$ is a yet unspecified body force. The third and fourth terms on the right-hand side of Eq. (1) constitute the Lorentz force. Equations (3) impose the incompressibility condition on the fluid and ensure the source-free property of the magnetic field. The body force $\mathbf{f}$ on the right-hand side of the NSE has to be specified in the concrete physical context and is the sum of all forces that drive the fluid, as e.g. the buoyancy force in thermal convection, or modify the motion, like the Coriolis force in a rotating star. For simplicity we restrict our investigation to the above system of MHD equations and do not include processes generating the forces. We consider $\mathbf{f}$ as externally applied and given. It pumps energy into the fluid and we look for long lasting magnetic fields, not decaying as a result of the nonlinear coupling of NSE and induction equation. This phenomenon will be called nonlinear dynamo effect.

Traditional dynamo theory has been mainly kinematic, i.e., the induction equation, Eq. (2), is solved for a prescribed velocity field, disregarding the equation of motion, Eq. (1). In the kinematic frame the question is whether a fluid motion can amplify, or at least prevent from decaying, some weak seed magnetic field. Solving the linear induction equation positive growth rates demonstrate an instability of the zero magnetic field solution and we speak of a kinematic dynamo effect. The ABC flow $\mathbf{v}_{\mathrm{ABC}}$ [4–6] (named after Arnold, Beltrami and Childress) and the Roberts flow $\mathbf{v}_{\mathrm{R}}$ [7,8] are intensively studied examples for dynamo-effective velocity fields.

To take into account the back reaction of the magnetic field on the velocity field, the kinematic analysis has to be extended to studying the full nonlinear MHD equations, Eqs. (1)–(3). The velocity fields $\mathbf{v}_{\mathrm{ABC}}$ and $\mathbf{v}_{\mathrm{R}}$ can be produced as steady solutions of the incompressible NSE, Eq. (1), if external body forces $\mathbf{f} = -\nabla^2\mathbf{v}_{\mathrm{ABC}}$ or $\mathbf{f} = -\nabla^2\mathbf{v}_{\mathrm{R}}$ are applied. These forces compensate viscous losses and generate the flows $R\mathbf{v}_{\mathrm{ABC}}$ or $R\mathbf{v}_{\mathrm{R}}$. Furthermore, together with a vanishing magnetic field, both flows are solutions of the full MHD equations, which are stable for small Reynolds numbers.

In this paper we report bifurcation studies of the MHD equations with the forcing types $\mathbf{f}_{\mathrm{ABC}}$ and $\mathbf{f}_{\mathrm{R}}$, respectively. Detailed results are published in Refs. [9–15] and are not all repeated here. We attempt to explain general properties of the nonlinear dynamo, but one has to keep in mind that there is still a large gap between the theoretical models and dynamos existing in nature. One of the most critical points is the magnitude of the Prandtl number $Pm = \nu/\eta$, the ratio between kinematic viscosity and magnetic diffusivity or, equivalently, between magnetic and kinetic Reynolds numbers. The Pm values occuring in cosmic dynamos cannot be reached by far in numerical simulations. For instance, the magnetic Prandl number in the convection zone of the Sun is of the order $10^{-4}\ldots10^{-6}$; in contrast, due to the numerical limitations, we set $Pm = 1$.

2 Dynamo bifurcations in the ABC flows

The most important branch of traditional kinematic dynamo theory is the theory of the turbulent dynamo. This is a mean-field theory where one averages over turbulently fluctuating parts of velocity and magnetic field. One of its central results is that the presence of kinetic helicity,

$$H_K = \mathbf{v}\cdot(\nabla\times\mathbf{v}), \tag{4}$$

in the fluctuating part of the velocity field is favourable for a dynamo effect. Here we consider non-turbulent or laminar helical dynamos (that is, no averaging is applied). In Sec. 2.1 the stronly helical pure ABC forcing is used. In Sec. 2.2 then the role of helicity for a dynamo effect is tested by imposing a generalized ABC forcing with a varying (i.e., parameter-dependent) degree of helicity.

2.1 Pure ABC forcing

One of the successful examples for producing a dynamo are the ABC flows, first investigated by Arnold [4],

$$\mathbf{v}_{\mathrm{ABC}} = (A\sin k_0 z + C\cos k_0 y, B\sin k_0 x + A\cos k_0 z, C\sin k_0 y + B\cos k_0 x), \tag{5}$$

where A, B, C denote constant coefficients and k_0 is a wave number. They are strongly helical Beltrami flows. Beltrami flows are flows with parallel velocity and vorticity $(\nabla\times\mathbf{v})$ vectors. The ABC flows satisfy the Beltrami condition,

$\nabla \times \mathbf{v} = \gamma \mathbf{v}$, with a constant γ, namely $\gamma = k_0$, which is a necessary condition for the existence of chaotic domains in Beltrami flows [4]. For this reason, they have received much interest [5,16], notably in the kinematic context as candidates for fast dynamos [6,17] (for which the growth rate remains bounded from below by a positive constant as the magnetic diffusivity tends to zero).

Imposing an external body force

$$\mathbf{f} = -\nabla^2 \mathbf{v}_{\mathrm{ABC}} = k_0^2 \mathbf{v}_{\mathrm{ABC}} \tag{6}$$

in the NSE and applying periodic boundary conditions with period 2π in all three spatial directions, Galanti et al. [18] investigated the system of MHD equations [Eqs. (1)–(3)]. Numerically simulating the system for different Reynolds numbers and selected initial conditions, they observed that at some critical value of the Reynolds number the ABC flow with no magnetic field loses stability to a time-periodic state in which a magnetic field is excited and which, thus, represents a dynamo.

At this stage we started our study of the ABC dynamo, for the special case $A = B = C = 1$, $k_0 = 1$, and describe here further transitions which finally lead to a chaotic dynamics. We applied bifurcation-analysis techniques and paid special attention to symmetry breakings. The magnetic Prandl number was set equal to unity, $Pm = Rm/R = 1$, so that the kinetic Reynolds number R was the only remaining control parameter. R was raised from zero in small steps in order that bifurcations were detected. For small R, there exists only one stable stationary solution, namely the ABC flow [given by Eq. (5)] with a vanishing magnetic field. Its symmetry group is the full equivariance group of the ABC forced MHD equations, the octahedral group O [4,19,16].

For varying R, this steady-solution branch was traced and the Jacobian matrix and its eigenvalues were computed in each step. The primary ABC flow loses stability in a Hopf bifurcation in which a stable periodic branch with a nonvanishing magnetic field is born. Since only a single pair of complex-conjugate eigenvalues crosses the imaginary axis, the new branch, denoted as period-1, retains the full symmetry O. More precisely, the solution is no longer point symmetric with respect to all symmetry transformations since some of these produce time shifts. However, the periodic orbit as a whole is invariant. In the table in Fig. 1 the solution branches detected, their region of stability and their symmetry are compiled. The numbers in the branch designations indicate the multiplicity of the branches, i.e., the number of coexisting conjugate branches. Per-3, for instance, stands for three coexisting branches of periodic solutions, each being invariant to one of three conjugate dihedral subgroups D_4. In the right half of the figure a schematic bifurcation diagram is depicted.

We do not want to explain all details in the bifurcation diagram, but note that there are two main (stable) branches. One of them is generated by successive bifurcations from the primary ABC flow. The other one, appearing with Per-3, seems to be a result of a saddle-node bifurcation; its unstable

Branch	Interval of stability for R	Symmetry
ABC flow	$0 < R < 5.7$	O
Per–1	$5.7 < R < 11.5$	O
Per–3	$7.7 < R < 16.0$	D_4
Per–4	$11.5 < R < 17.3$	D_3
Torus–3	$16.0 < R < 20.0$	
Torus–4	$17.3 < R < 17.9$	
Chaos–3	$R \geq 20.0$	
Chaos–4	$R \geq 17.9$	

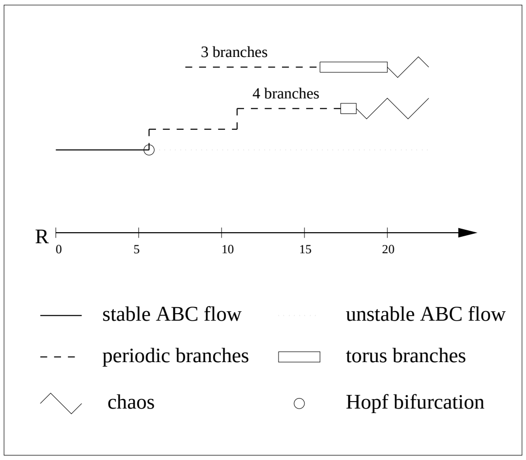

Fig. 1. Overview of the different solution branches (left). Schematic bifurcation diagram (right).

counterpart has not been found. Starting from random initial conditions the trajectory is nearly always attracted by these solutions. Obviously, the basin of attraction of the first main branch shrinks for increasing values of R. Quasiperiodic solutions, briefly denoted as tori, and final transitions to chaos were observed for both main branches. The chaoticity of the solutions was verified by calculating the largest Lyapunov exponents. For this purpose an algorithm by Shimada and Nagashima [20] was implemented. Fig. 2 shows the cumulative values of the five largest Lyapunov exponents versus the integration time. It demonstrates good convergence of the algorithm also in applications to high-dimensional systems of ordinary differential equations as resulting from our Galerkin approximation to the original partial differential equations. It is seen that at least one of the exponents is positive.

Next we want to give an impression of the magnetic field structure in real (configuration) space and its changes under the influence of symmetry breaking bifurcations. In a kinematic dynamo study using the ABC flow with $A = B = C$, Galloway and Frisch [21] were the first to observe cigar-like concentrations of the magnetic field about velocity stagnation points. The ABC flow for the case $A = B = C$ has eight stagnation points, which are unstable fixed points of the flow $\mathbf{v}$. The corresponding eigenvalues are real and have signs $(+,-,-)$ or $(-,+,+)$. The topological structure of the ABC flow, and in particular the intersections of the stable and unstable manifolds of the stagnation points, which form a complicated web of heteroclinic lines, were comprehensively discussed by Dombre et al. [16]. Stagnation points with a two-dimensional stable manifold have been denoted as of α type

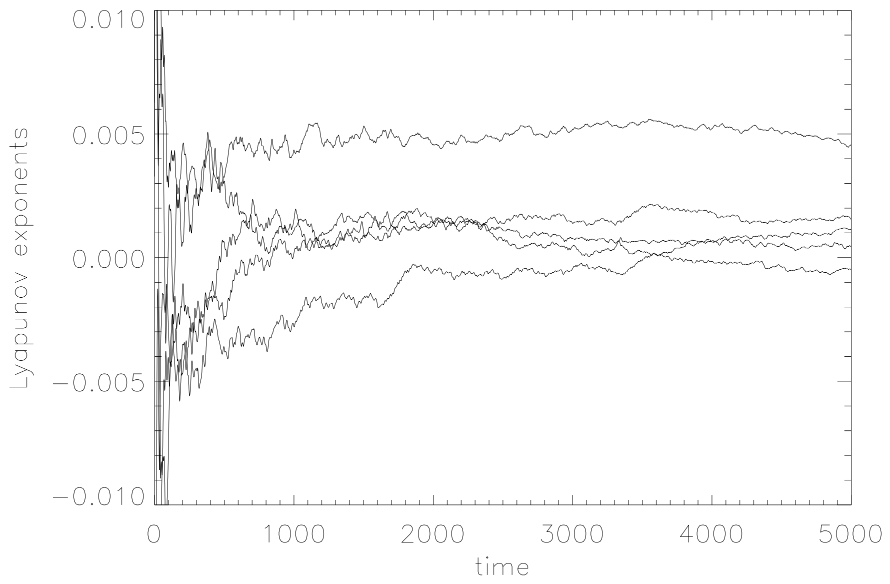

Fig. 2. The five largest Lyapunov exponents versus integration time for the branch Chaos-3 at $R = 20$.

and those with a two-dimensional unstable manifold as of β type. There are four stagnation points of each type and any two points of different type are connected by a straight line, forming a one-dimensional heteroclinic orbit. The cube diagonal through the points $(0, 0, 0)$ and $(2\pi, 2\pi, 2\pi)$, for example, is a one-dimensional invariant manifold belonging to the stagnation points $(3\pi/4, 3\pi/4, 3\pi/4)$ (β type) and $(7\pi/4, 7\pi/4, 7\pi/4)$ (α type). The rest of the ensemble of stagnation points and associated one–dimensional invariant manifolds can be obtained by applying symmetry transformations of the original equivariance group. The cigar-like structures of the magnetic field, observed by Galloway and Frisch [21] as well as by Galanti et al. [18] for the kinematic problem, are localized about the stagnation points of the α type.

Immediately after the primary Hopf bifurcation, where the ABC flow loses stability and a magnetic field appears, one expects the flow to differ only weakly from the unperturbed ABC flow and the magnetic field to resemble the unstable eigenmode of the kinematic problem. Above we already mentioned that the bifurcation retains the original symmetry for the newly created periodic branch Per–1. This symmetry has also a decisive influence on the spatial structure of the corresponding magnetic and velocity fields, here briefly discussed. A surprising feature of the new branch is that the eight stagnation points of the ABC flow survive, i.e., they remain time-independent zero-velocity points at the same location as before for the original ABC flow. In Fig. 3 isosurfaces of the magnetic field strength for a level of 65% of the maximum value are drawn. The cigar-like structure are clearly recognizable

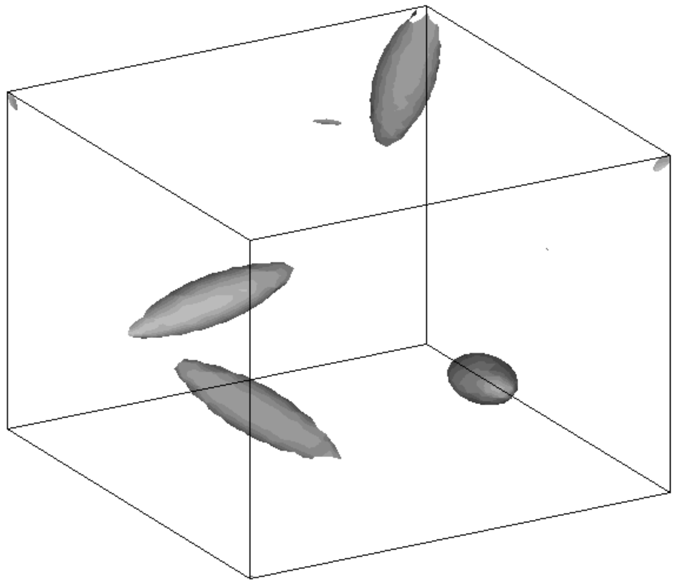

Fig. 3. Isosurfaces of the magnetic field with 65% of the maximal modulus for the symmetric branch (R=10) in the periodic box (x,y,z between 0 and 2π).

also in the nonlinear regime. Due to the temporal periodicity, the magnetic field oscillates and the shape of the isosurfaces depends also on the time at which a snapshot is made; sometimes they look much more like blobs. To give an impression of the dynamics, we consider the fields on the diagonal line. As already mentioned, the stagnation points remain unchanged, but furthermore also their invariant one-dimensional manifolds are formed by the same straight lines as before. For the diagonal line, containing two stagnation points, this follows directly from the symmetry of the branch. Namely, as a consequence of the symmetry with respect to the cyclic group Z_3 as a subgroup of the full symmetry group, the velocity field has to be aligned with the diagonal direction. The same holds for the magnetic field.

In Fig. 4 the magnetic field component along the diagonal line is shown for different instants of a time period (stagnation points are marked by asterisks). Strong oscillations with a large amplitude occur around the stagnation point of α type, and the magnetic energy is mainly located in its neighborhood. The

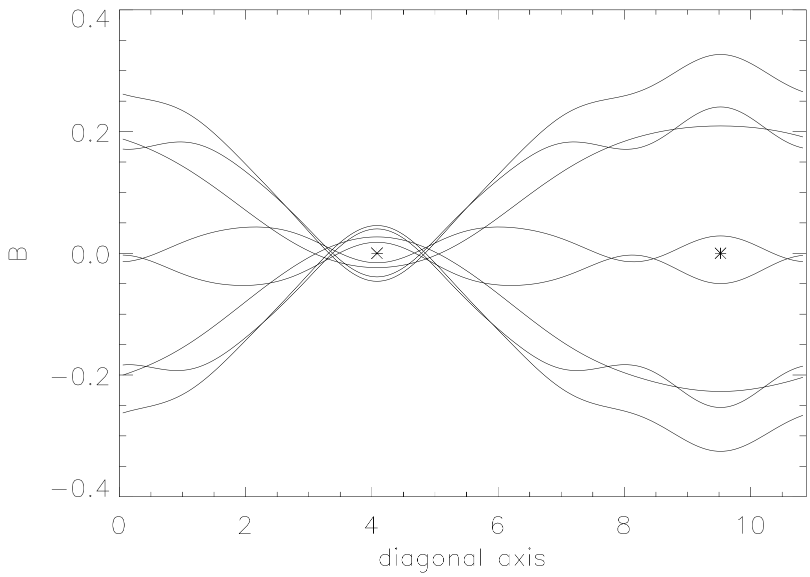

Fig. 4. Magnetic field component along the diagonal axis at different instants of time (R=10). Stagnation points are marked by asterisks.

velocity field along the diagonal line oscillates only relatively weakly about the original ABC flow.

It is not our aim here to describe the structural properties of the magnetic field for all branches presented in Fig. 1. We only mention an interesting property of the chaotic branch Chaos–3: Also for this branch the magnetic energy is on average mainly concentrated in four tube-like structures. These oscillate and move irregularly through the cube. The appearance of just four strong-field regions is still reminiscent of the four α type stagnation points of the original ABC flow.

2.2 Generalized ABC forcing with varying helicity

In order to test the role of helicity for a dynamo effect we have, besides the pure ABC forcing given by Eq. (5), also applied a generalized ABC forcing of the form

$$\mathbf{f} = (1-\lambda)\mathbf{v}_{ABC} + \lambda \mathbf{v}^{-}_{ABC}, \tag{7}$$

where we introduce

$$\mathbf{v}^{-}_{ABC} = (A\cos k_0 z + C\sin k_0 y,\ B\cos k_0 x + A\sin k_0 z,\ C\cos k_0 y + B\sin k_0 x) \tag{8}$$

and λ is a parameter varying between 0 and 0.5 (but $A = B = C = k_0 = 1$ in all calculations described here). $\mathbf{v}^{-}_{ABC}$ satisfies $\nabla \times \mathbf{v}^{-}_{ABC} = -k_0 \mathbf{v}^{-}_{ABC}$ and for a positive k_0 its helicity is thus negative whereas that of the original ABC flow is positive. The degree of helicity in the forcing varies with λ. For $\lambda = 0.5$ the addition of $\mathbf{v}^{-}_{ABC}$ in the forcing term "kills" the helicity on average in the volume while $\lambda = 0$ corresponds to the original ABC forcing.

We now present the bifurcation diagram obtained when applying the generalized ABC forcing, given by Eq. (7). For weak forcing (small R), there exists always a stable stationary, globally attracting solution (which coincides with the original ABC flow only in the special case of $\lambda = 0$). Keeping λ fixed and raising R, we have traced the steady-solution branch. For $\lambda < 0.4$ the steady state loses stability in a Hopf bifurcation, but at $\lambda = 0.4$ the type of the first bifurcation, as well as the character of the time-asymptotic states after this bifurcation, change. While for $\lambda < 0.4$ a magnetic periodic state is the (only) new attractor, for λ between 0.4 and 0.5 new non-magnetic states appear.

The original steady state has been traced also in the region beyond the first bifurcation, where it is unstable and where it undergoes secondary bifurcations. The locations of primary and secondary bifurcations in the parameter plane are shown in Fig. 5. Thick solid and dashed lines, respectively, indicate the primary bifurcation of the original steady state. For $0.4 < \lambda < 0.49$ the Hopf bifurcation is preceded by a bifurcation in which two real eigenvalues of the Jacobian matrix become positive; these two eigenvalues are equal already before the bifurcation, due to one of the symmetries in the system. The bifurcation results in three coexisting new stable stationary solutions, which can

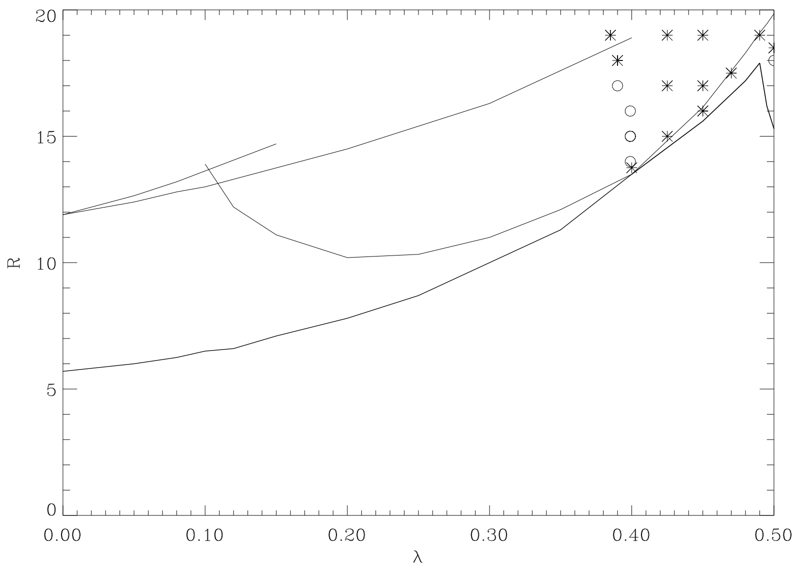

Fig. 5. Locations of primary and secondary bifurcations of the original stationary solution in the λ-R plane. Solid line and dashed-dotted line: a single pair of complex conjugate eigenvalues crosses the imaginary axis; dashed line: two real eigenvalues pass through zero; dotted line: two pairs of complex conjugate eigenvalues cross the imaginary axis. Asterisks indicate points at which, by means of simulations, non-magnetic chaotic (Shilnikov-like) time-asymptotic states have been found, while circles correspond to magnetic periodic attractors.

be transformed into each other by certain elements of the symmetry group of the problem (which is a subgroup of the symmetry group O in the case of the pure ABC forcing). For $\lambda = 0.4$ this bifurcation occurs simultaneously with the Hopf bifurcation.

At $\lambda = 0.49$, showing up as a kind of cusp in Fig. 5, the primary bifurcation changes its character again, namely from the real bifurcation observed for $\lambda < 0.49$ to another Hopf bifurcation for $\lambda > 0.49$. This Hopf bifurcation leads to a non-magnetic periodic state. At the cusp-like transition point the imaginary part of the pair of complex-conjugate eigenvalues responsible for the Hopf bifurcation to the right is zero, and the complex-conjugate pair coincides with the real pair responsible for the bifurcation to the left.

The new stationary and periodic solutions bifurcating from the original stationary one for $0.4 < \lambda < 0.5$ are stable only over very small intervals of the bifurcation parameter R and lose their stability directly to non-magnetic chaotic states. The presence of chaos has again been verified by calculating, for selected values of the bifurcation parameters, the largest Lyapunov exponents.

The chaotic attractors found here are strongly suggestive of Shilnikov-type homoclinic chaos. In a three-dimensional flow, this type of chaos is related to the existence of a homoclinic trajectory to a saddle point with a real eigenvalue and a pair of complex-conjugate eigenvalues, the real eigenvalue having a larger magnitude than the real part of the complex eigenvalues (cf. Ref. [22], Sec. 6.5.). The trajectory shown in Fig. 6 seems to be very close to such a homoclinic orbit. It approaches the unstable fixed point along a path apparently close to a one-dimensional stable manifold, spirals outward (thereby seemingly close to a two-dimensional unstable manifold), approaches again the fixed point, and so on. In our case the phenomenon seems to be connected with the degenerate bifurcation at $\lambda = 0.4$ (crossing of solid and dashed line in Fig. 5). In problems with two parameters, the occurence of homoclinic orbits in the vicinity of such points of degeneracy is a generic phenomenon (see e.g. Ref. [23]).

In Fig. 5, asterisks indicate points at which non-magnetic Shilnikov-like chaotic attractors have been found. The non-magnetic chaotic domain extends also to λ values less than 0.4, there causing a disappearance of the dynamo effect already present at smaller Reynolds numbers.

To repeat the main result of the studies using the generalized ABC forcing: In order that the primary bifurcation leads to a dynamo, the degree of helicity in the forcing has to exceed a threshold value.

3 Dynamo effect in convection-like rolls

In this section we treat another dynamo model and compare it with the ABC dynamo in order to get further insight into the magnetic field generation mechanisms. It is based on a flow introduced by G. O. Roberts [7,8]. The

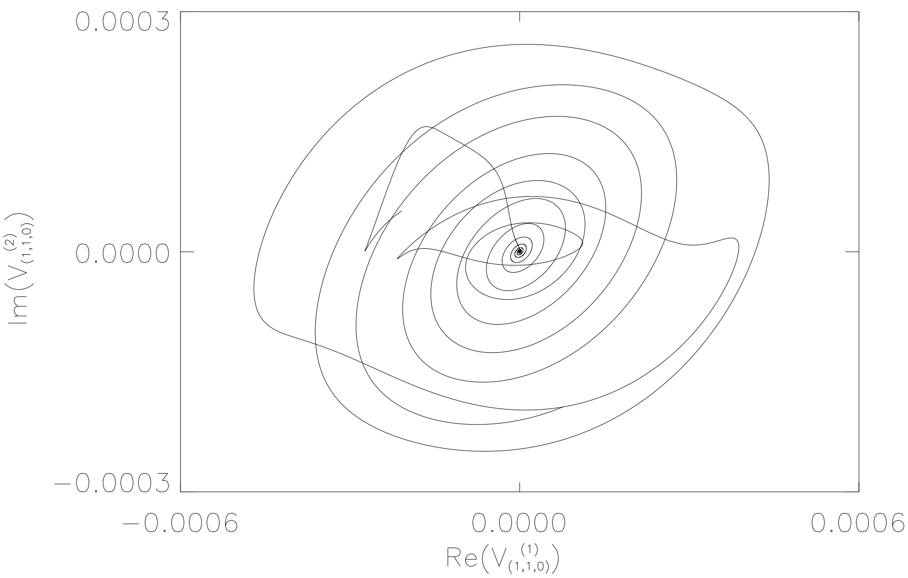

Fig. 6. Projection of a trajectory onto the plane spanned by two of the velocity components for $\lambda = 0.45$ and $R = 15.7$.

Roberts flow has recently received renewed interest. On one hand it resembles the roll solutions of thermal (or solutal) convection. In the convective zones of rotating celestial bodies, for instance, convection rolls parallel to the axis of rotation tend to be formed [24]. On the other hand the Roberts flow is approximately realized in an ongoing laboratory experiment aimed at demonstrating the dynamo effect under laboratory conditions [25,26]. The experimental setup has been motivated by the kinematic dynamo effectiveness of the Roberts flow and its supposed resemblance to planetary convection. A conducting fluid (sodium) is pumped through an array of straight parallel ducts which are connected at their ends, where the flow out of a duct reverses its direction before entering a neighboring duct. The ducts contain internal guiding structures such that the flow becomes helical. All guiding structures, including the (thin) walls separating neighboring ducts, are electrically conducting.

Kinematic studies related to this experiment are due to Apel et al. [27] and Tilgner [28]. Apel et al. applied mean-field dynamo theory [2], whose central mechanism is the alpha effect (the generation of a mean electromotive force parallel to the mean magnetic field by turbulent fluctuations of velocity and magnetic field), while Tilgner used direct numerical simulation of the induction equation. In both studies the prescribed flow was the Roberts flow and system parameters most suitable for dynamo excitation were determined. But due to the kinematic nature of the models used the feedback of the magnetic field to the velocity field remained an open problem. This gave us the motivation to study bifurcations of the MHD equations for the situation where an external forcing of the Roberts type is applied.

The Roberts flow is given as a family of three-dimensional velocity fields which are independent of one of the spatial coordinates, namely,

$$\mathbf{v}_{\mathrm{R}} = (g \sin x \cos y,\ -g \cos x \sin y,\ 2f \sin x \sin y). \tag{9}$$

f and g are parameters, but we have only used $f = g = 1$ in our calculations. The flow consists of an array of rolls where the fluid spirals up and down in neighboring rolls. To give an impression of the flow structure, a projection of the velocity vectors on the x-y plane is plotted in Fig. 7. Since the flow is periodic with period 2π in the x and y directions, we consider only the four rolls shown. Applying analogously to Eq. (6) now the external forcing $\mathbf{f} = -\nabla^2 \mathbf{v}_{\mathrm{R}} = 2\mathbf{v}_{\mathrm{R}}$, the Roberts flow with vanishing magnetic field is a solution of the full MHD equations [Eqs. (1)–(3)]. It is also the only time-asymptotic steady-state for small R ($Pm = Rm/R$ is again fixed to the value 1). As in the case of the ABC forcing, we applied periodic boundary conditions with period 2π in all three spatial directions.

For increasing Reynolds number a sequence of bifurcations occurs. Fig. 8 shows the stable solution branches that we obtained by applying continuation techniques and additional simulations. The sudden drop of the magnetic energy in the transition from periodic to quasiperiodic dynamics is conspicuous. For an explanation of this phenomenon we refer to [15] where also a

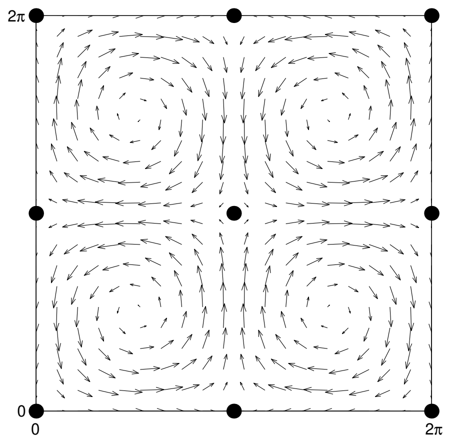

Fig. 7. Projection of the Roberts flow on the x-y plane. Black points indicate stagnation points of the flow.

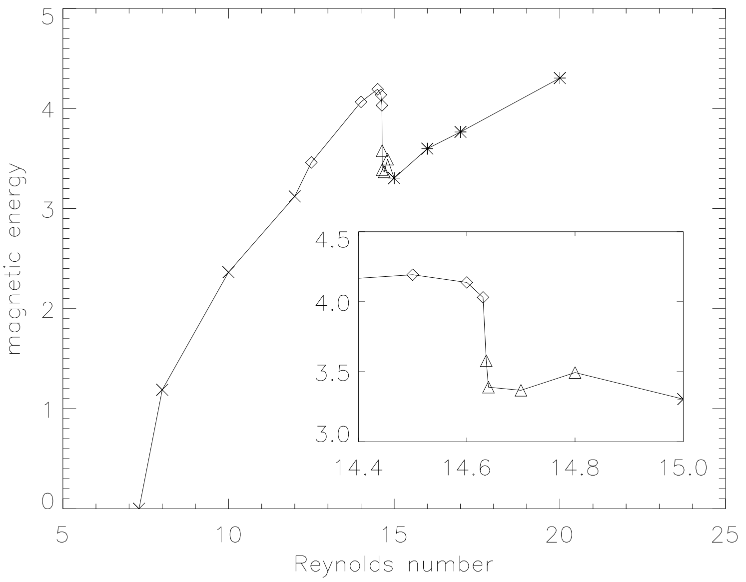

Fig. 8. Magnetic energy versus Reynolds number. Steady-state ($\times$), periodic ($\diamond$), torus ($\triangle$), and chaotic solutions ($*$) are marked. The inner small box shows the zoomed region for $R = 14.4 \ldots 15.0$.

discussion of the route to chaos may be found. Here we concentrate on the role of symmetry breaking for the onset of the dynamo and for the spatial structure of the generated magnetic field.

The external forcing, or equivalently its defining flow $\mathbf{v}_{\mathrm{R}}$, determines essentially, but not completely, the equivariance group of the MHD equations. The Roberts flow, given by Eq. (9), is invariant with respect to symmetry transformations forming a group which is the direct product of a discrete group G with the circle group S^1. But additionally a reflection symmetry Z_2 corresponding to the transformation $\mathbf{B} \to -\mathbf{B}$ and $\mathbf{v} \to \mathbf{v}$ leaves the MHD equations invariant. It plays an essential role in the symmetry breaking bifurcations and has to be taken into account. Thus, the whole equivariance group can be written as

$$G \times S^1 \times Z_2. \tag{10}$$

The forcing term, defined by $\mathbf{v}_{\mathrm{R}}$, is independent of the z coordinate. This provides together with imposed periodic boundary conditions the circle symmetry S^1. The discrete group G is also determed by the flow $\mathbf{v}_{\mathrm{R}}$. It consists of sixteen elements and can be characterized as a semidirect product $D_2 \times_S Z_4$. The dihedral group D_2 is the group of rotations about the x, y and z axes by π and forms a normal subgroup. The group Z_4 is generated by a rotation about the z axis by $\pi/2$ with an additional shift by π in the x direction. Applying rotations about the z axis (see Fig. 7) it has to be taken into account that the flow has a nonvanishing z component and neighboring vortices spiral in opposite directions. Thus, these rotations by $\pi/2$ have to be combined with a shift by π. Nevertheless the group is isomorphic to Z_4.

Now we analyze the first symmetry breaking bifurcation (see Fig. 8) in which the primary branch, the Roberts flow, becomes unstable and a nonvanishing magnetic field appears. At this bifurcation point two eigenvalues which belong to magnetic modes are equal to zero. The symmetry breaking pitchfork bifurcation yields new steady states representing stationary dynamos. The original symmetry is broken, namely, the solutions are no longer S^1 invariant. Now both the magnetic and the velocity fields depend on the z coordinate. The discrete symmetry $(D_2 \times_S Z_4) \times Z_2$ survives but is now formed by other transformations than before. The Z_4 symmetry generated by the rotation about the z axis and the shift in the x direction has now to be combined with an additional translation in the z direction by $\pi/2$, a remnant of the S^1 symmetry. The reflection symmetry Z_2 corresponding to the transformation $\mathbf{B} \to -\mathbf{B}$ and $\mathbf{v} \to \mathbf{v}$ has also to be combined with a translation in the z direction, namely by π.

Furthermore, the action of D_2 has become more subtle. Before giving this action, we characterize the stagnation points of the Roberts flow and the perturbed velocity field after the bifurcation. The stagnation points of $\mathbf{v}_{\mathrm{R}}$ are indicated in Fig. 7. Due to its independence of the z coordinate, the flow possesses continuous lines of stagnation points which are connected by a family of heteroclinic orbits. The symmetry breaking bifurcation splits up these lines into a discrete set of sixteen stagnation points. A skeleton of the stagnation points together with the connecting heteroclinic orbits after the bifurcation is sketched in Fig. 9 (for counting the stagnation points the periodicity has to be taken into account). There are eight stagnation points

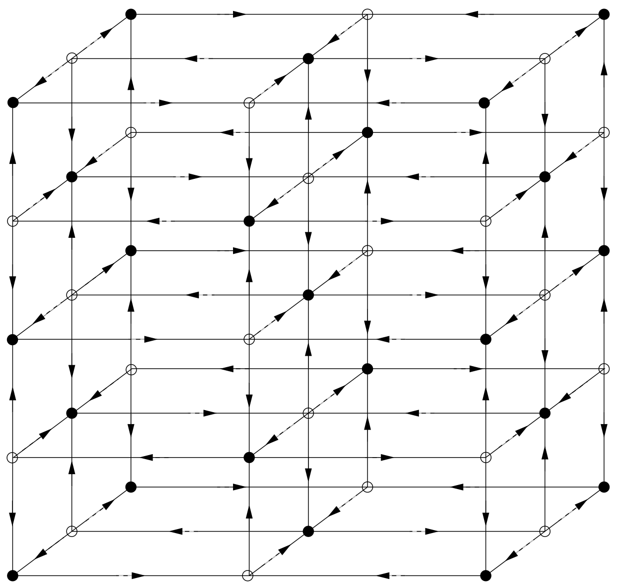

Fig. 9. Stagnation points and their connecting heteroclinic orbits after the first bifurcation. Black dots: α-type stagnation points. White dots: β-type stagnation points.

with two negative eigenvalues and one positive eigenvalue (α type) and eight points with opposite signs of the eigenvalues (β type). The symmetry breaking bifurcation produces a family of equivalent solutions which differ only by translations in the z direction. We select one of them by choosing the coordinates $x = y = z = 0$ for one of the α-type stagnation points. Fig. 9 also helps to get a better understanding of the Z_4 symmetry described above, in particular of the necessary incorporation of translations by $\pi/2$ in the z direction as a result of the broken S^1 symmetry. But now we shall explain the actions of the surviving D_2 symmetry, one of the conjugate subgroups with respect to which the special solution branch shown in Fig. 9 is invariant. These actions are rotations by π about the x, y or z axis, combined with additional reflections $\mathbf{B} \to -\mathbf{B}$ of the magnetic field for rotations about the x or z axis (but without such a reflection for the rotation about the y axis). Obviously, these transformations form really a D_2 group.

Finally, we describe the magnetic field generated by this bifurcation. We observed that the magnetic field is strongly amplified in the neighborhood of stagnation points of the β type, which have a one-dimensional stable and a two-dimensional unstable manifold. Plotting level surfaces of the magnetic field strength similar to Fig. 3, potato-like structures around the β-type stagnation points became visible. It is a prevalent guess that the stagnation points and, especially, the chaotic structure of the underlying flow in their vicinity, promote the dynamo effect. Therefore, we investigated the structure of the velocity field by a bunch of passive tracers which were initially randomly distributed in the periodic cube. Figure 10 shows Poincaré sections of the flow for one helical roll, with the x-y plane at z=0 and the x-z plane at y=$\pi/2$, respectively, as cutting planes. One recognizes the regular structure

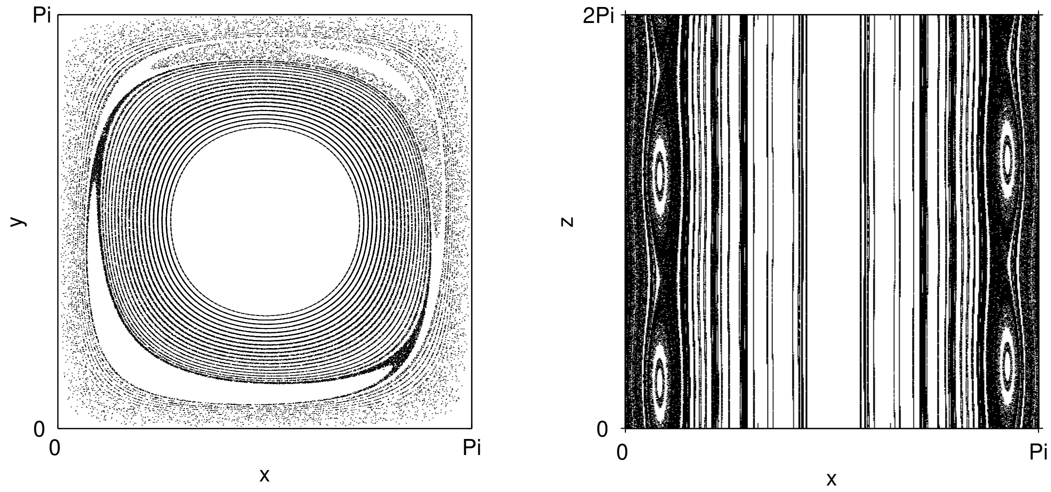

Fig. 10. Poincaré sections of the velocity field after the symmetry breaking bifurcation. Cutting planes are the x-y plane at z=0 (left) and the x-z plane at y=$\pi/2$ (right).

of the driven helical rolls and a chaotic region with some surviving KAM tori. Inside the helical rolls the strength of the produced magnetic field is really substantially weaker than in the chaotic region, a phenomenon which supports the above conjecture.

4 Concluding remarks and outlook

We have demonstrated the dynamo effect by means of two examples in which the fluid was driven by two different types of external forcing. The forcing terms in turn were motivated by the kinematic dynamo properties of two flows, the ABC flow and the Roberts flow, respectively. We want to conclude here with a discussion of some similarities and some differences between the two models.

The ABC flow is a chaotic flow from the beginning and causes a stretching, folding and twisting of the magnetic field lines, a process which is an effective drive of a dynamo [29]. Because of the chaoticity of the primary ABC flow it is conjectured, but not proved yet, that the ABC dynamo is a fast dynamo [30]. This notion, originally defined for the kinematic problem, means that the dynamo mechanism is independent of the magnetic diffusivity and works in principle also in the limit of a perfectly conducting fluid. The first bifurcation of the ABC forced system is a symmetry preserving Hopf bifurcation generating solutions that depend periodically on time. Concentrations of the magnetic energy are found around the stagnation points of the α type, which have two-dimensional stable and one-dimensional unstable manifolds and which survive the bifurcation. The mechanism of stretching, twisting and folding, which works in their vicinity, thus continues to operate in the nonlinear regime.

Unlike the ABC flow, the Roberts flow is regular. Its stagnation points fill lines and the flow around them is non-chaotic. Therefore, the mechanism of stretching, twisting and folding is missing here and the kinematic Roberts dynamo is probably not a fast dynamo. Instead, the shearing motion between counter-rotating neighboring rolls is responsible for the kinematic dynamo effect. However, isolated stagnation points and chaotic stream lines are generated in the first bifurcation. As for the ABC flow, we got evidence that the chaoticity is caused by a complex web of heteroclinic lines formed by intersections of two-dimensional stable and unstable manifolds of the stagnation points. Furthermore, the magnetic field is concentrated in chaotic flow regions. Is then perhaps the nonlinear Roberts dynamo basically different from the kinematic one? The maximal amplification of the magnetic field occurs in the vicinity of the β-type rest points where the stretch-twist-fold mechanism is believed not to work. Thus it remains unclear whether the chaoticity of the flow is essential for the dynamo or merely a by-product. This will have to be clarified in future investigations. A next step could be a kinematic dynamo study with the stationary velocity field generated in the first bifurcation as prescribed flow, in order to see whether this flow remains dynamo effective for high magnetic Reynolds numbers. The latter would be indicative of a decisive role of chaotic stretching.

References

1. H. K. Moffatt. *Magnetic Field Generation in Electrically Conducting Fluids.* Cambridge Univ. Press, Cambridge, 1978.
2. F. Krause and K.-H. Rädler. *Mean-Field Magnetohydrodynamics and Dynamo Theory.* Akademie-Verlag, Berlin, 1980.

3. P. H. Roberts and A. M. Soward. Dynamo theory. *Ann. Rev. Fluid Mech.*, 24:459–512, 1992.
4. V. I. Arnold. Sur la topologie des êcoulements stationnaires des fluides parfaits. *C. R. Acad. Sci. Paris*, 261:17–20, 1965.
5. V. I. Arnold and E. I. Korkina. The growth of a magnetic field in a three-dimensional steady incompressible flow (in Russian). *Vest. Mosk. Univ. Mat. Mekh.*, 3:43–46, 1983.
6. D. Galloway and U. Frisch. Dynamo action in a family of flows with chaotic streamlines. *Geophys. Astrophys. Fluid Dyn.*, 36:53–83, 1986.
7. G. O. Roberts. Spatially periodic dynamos. *Phil. Trans. Roy. Soc.*, 266:535–558, 1970.
8. G. O. Roberts. Dynamo action of fluid motions with two-dimensional periodicity. *Phil. Trans. Roy. Soc.*, 271:411–454, 1972.
9. F. Feudel, N. Seehafer, and O. Schmidtmann. Fluid helicity and dynamo bifurcations. *Phys. Lett. A*, 202:73–78, 1995.
10. F. Feudel, N. Seehafer, and O. Schmidtmann. Bifurcation phenomena of the magnetofluid equations. *Math. Comput. Simulat.*, 40:235–245, 1996.
11. N. Seehafer, F. Feudel, and O. Schmidtmann. Nonlinear dynamo with ABC forcing. *Astron. and Astrophys.*, 314:693–699, 1996.
12. F. Feudel, N. Seehafer, B. Galanti, and S. Rüdiger. Symmetry-breaking bifurcations for the magnetohydrodynamic equations with helical forcing. *Phys. Rev. E*, 54:2589–2596, 1996.
13. O. Schmidtmann, F. Feudel, and N. Seehafer. Nonlinear Galerkin methods for the 3D magnetohydrodynamic equations. *Int. J. Bifurcation and Chaos*, 7:1497–1507, 1997.
14. O. Schmidtmann, F. Feudel, and N. Seehafer. Nonlinear Galerkin methods based on the concept of determining modes for the magnetohydrodynamic equations. *J. Phys. A: Math. Gen.*, 31:7141–7155, 1998.
15. S. Rüdiger, F. Feudel, and N. Seehafer. Dynamo bifurcations in an array of driven convection-like rolls. *Phys. Rev. E*, 57:5533–5538, 1998.
16. T. Dombre, U. Frisch, J. M. Greene, M. Hénon, A. Mehr, and A. M. Soward. Chaotic streamlines in the ABC flows. *J. Fluid Mech.*, 167:353–391, 1986.
17. B. Galanti, A. Pouquet, and P. L. Sulem. Influence of the period of an ABC flow on its dynamo action. In M. R. E. Proctor, P. C. Matthews, and A. M. Rucklidge, editors, *Theory of Solar and Planetary Dynamos*, pages 99–103. Cambridge University Press, Cambridge, 1993.
18. B. Galanti, P. L. Sulem, and A. Pouquet. Linear and non-linear dynamos associated with ABC flows. *Geophys. Astrophys. Fluid Dyn.*, 66:183–208, 1992.
19. V. I. Arnold. On the evolution of a magnetic field under the influence of advection and diffusion (in Russian). In V. M. Tikhomirov, editor, *Some Problems of Modern Analysis*, pages 8–21. Moscow State University, Moscow, 1984.
20. I. Shimada and T. Nagashima. A numerical approach to ergodic problem of dissipative dynamical systems. *Progr. Theor. Phys.*, 61:1605–1616, 1979.
21. D. Galloway and U. Frisch. A note on the stability of a family of space-periodic Beltrami flows. *J. Fluid Mech.*, 180:557–564, 1987.
22. J. Guckenheimer and P. Holmes. *Nonlinear Oscillations, Dynamical Systems, and Bifurcations of Vector Fields.* Springer, New York, 1983.
23. G. Nicolis and P. Gaspard. Bifurcations, chaos and self-organisation in reaction-diffusion systems. In D. Roose, B. de Dier, and A. Spence, editors, *Continuations and Bifurcations: Numerical Techniques and Applications*, pages 43–70. Kluwer, Dordrecht, 1990.

24. F. H. Busse. Convection driven zonal flows and vortices in the major planets. *Chaos*, 4:123–124, 1994.
25. R. Stieglitz and U. Müller. GEODYNAMO — Eine Versuchsanlage zum Nachweis des homogenen Dynamoeffektes. Research Report FZKA-5716, Forschungszentrum Karlsruhe, 1996.
26. F.H. Busse, U. Müller, R. Stieglitz, and A. Tilgner. Spontaneous generation of magnetic fields in the laboratory. In F.H. Busse and S.C. Müller, editors, *Evolution of Spontaneous Structures in Dissipative Continuous Systems*, Lecture Notes in Physics, pages 546–558. Springer-Verlag, Berlin, 1998.
27. A. Apel, E. Apstein, K.-H. Rädler, and M. Rheinhardt. Contributions to the theory of the Karlsruhe dynamo experiment. Research Report, Astrophysikalisches Institut Potsdam, 1996.
28. A. Tilgner. A kinematic dynamo with a small scale velocity field. *Phys. Lett. A*, 226:75–79, 1997.
29. S. Childress and A.D. Gilbert. *Stretch, Twist, Fold: The Fast Dynamo.* Lecture Notes in Physics. Springer, Berlin, 1995.
30. A.M. Soward. Fast dynamos. In M. R. E. Proctor and A.D. Gilbert, editors, *Theory of Solar and Planetary Dynamos*, pages 181–217. Cambridge University Press, Cambridge, 1994.